Chemical Engineering Journal 193-194 (2012) 39–49

Contents lists available at SciVerse ScienceDirect

Chemical Engineering Journal

journal homepage: www.elsevier.com/locate/cej

Removal of organic materials from TNT red water by Bamboo Charcoal adsorption

Dan Fu [a,b], Yihe Zhang [a,c,*], Fengzhu Lv [a], Paul K. Chu [c], Jiwu Shang [a]

[a] State Key Laboratory of Geological Processes & Mineral Resources, National Laboratory of Mineral Materials, School of Materials Sciences and Technology, China University of Geosciences, Beijing 100083, China
[b] Department of chemistry, Liaoning Petrol Chemical Vocational College, Liaoning 121001, China
[c] Department of Physics & Materials Science, City University of Hong Kong, Tat Chee Avenue, Kowloon, Hong Kong, China

ARTICLE INFO

Article history:
Received 10 January 2012
Received in revised form 13 March 2012
Accepted 14 March 2012
Available online 30 March 2012

Keywords:
Adsorption
Bamboo-charcoal
Organic materials
TNT red water

ABSTRACT

Bamboo Charcoal (BC) was used as an adsorbent to remove organic materials from TNT red water. The studies were carried out by varying pH, dilution ratios of TNT red water, contact time and temperature. The characterizations of BC were analyzed by N_2 adsorption, Boehm titration method, mass titration, the scanning electronic microscopy (SEM), X-ray diffraction (XRD) and Fourier transform infrared spectroscopy (FTIR). The functional groups of TNT red water was also determined by FTIR. The equilibrium adsorption data were analyzed using Langmuir, Freundlich, Temkin and Dubinin–Radushkevich (D–R) isotherms. It was observed that the Langmuir isotherm fitted the experimental results well and the adsorption involved a physical mechanism by the D–R models analysis. The pseudo-second-order kinetic model described the adsorption kinetics of the organic materials from TNT red water very well. The studies of external diffusion and intraparticle diffusion models showed that external as well as intraparticle diffusion also influenced on the actual adsorption process. Thermodynamic studies showed that the adsorption of organic materials from TNT red water on BC was a spontaneous, endothermic process and the randomness increases at the solid/solution interface. The mechanisms of adsorption were studied by electrostatic interactions, hydrogen bonding formation electron, donor–acceptor interaction and π–π dispersion interaction.

1. Introduction

Millions of tons of nitro-aromatic explosives are used annually in military and civilian related activities and the most widely used explosive is 2,4,6-trinitrotoluene (TNT) [1]. A large amount of wastewater is generated during TNT production and according to the characteristic color, it can be classified as TNT red water, yellow water, pink water and condensates [2]. TNT red water which is produced during manufacturing and refining of TNT has complex compositions and is toxic, carcinogenic, mutagenic, and not easily biodegraded [3]. The TNT red water, if untreated, contaminates soil and underground water affecting the health of humans and bringing serious environmental problems. There are many methods to remove TNT and other organic materials from wastewater, for example, adsorption [4,5], extraction [6], oxidation by UV/H_2O_2 [7], photo-catalytic oxidation [8], Fenton reagent oxidation [9] and biological methods [10]. Adsorption is one of the commonly used methods but adsorbents can be expensive and there is much research on developing more efficient and economical adsorbents to treat TNT red water.

Some recent studies have focused on biomass resource as the adsorbent. It is highly efficient and inexpensive [11]. Among the various types of biomass resources, bamboo is recognized as one of the most popular ones because of its abundance, especially in China, short growth cycle, renewability, simple production, and low price. Bamboo Charcoal (BC), a main product of bamboo manufacturing, is a novel biomass adsorbent which has strong adsorption ability for organic pollutants [12–14]. However, there has not been much work on using the materials to remove organic materials from TNT red water. The objective of this work is to evaluate systematically adsorption of organic materials from TNT red water by using BC. The effects of pH, dilution ratios of TNT red water, contact time and temperature on adsorption characteristics as well as the adsorption mechanism are studied.

2. Experimental

2.1. Materials and methods

2.1.1. Adsorbent

BC was supplied by the Chinese Academy of Forestry, Beijing, China. BC was washed with distilled water to remove impurities, oven dried at 378 K, and kept in a vacuum desiccator for further

* Corresponding author. Tel./fax: +86 10 82323433.
E-mail address: zyh@cugb.edu.cn (Y. Zhang).

1385-8947/$ - see front matter Crown Copyright © 2012 Published by Elsevier B.V. All rights reserved.
http://dx.doi.org/10.1016/j.cej.2012.03.039

Table 1
The results of Boehm's titration before and after adsorption, pH_{pZC} and the N_2 adsorption isotherm of BC.

Parameter	The value before adsorption (mmol/g)		The value after adsorption (mmol/g)
Carboxylic groups	0.2525		0.2076
Phenolic groups	0.1821		0.1410
Lactonic groups	0.1605		0.1327
Acid groups	0.5951		0.4813
Basic groups	0.5765		0.1860
pH_{PZC}		8.21	
BET		303.94 m^2/g	
Pore volume		0.2079 cm^3/g	
Average pore diameter		2.74 nm	

use. The surface area, pore volume and average pore diameter of BC were measured by N_2 adsorption isotherm using an ASAP 2020 Micromeritics instrument. The surface functional groups of BC before and after adsorption were investigated by Boehm's titration [15]. The point of zero charge (pH_{PZC}), which is the pH value required to give zero net surface charge, was determined by a mass titration method proposed by Noh and Schwarz [16]. The pH was measured by a pH meter (pHSJ-4A, Shanghai, China).The results of characterization are shown in Table 1.

The Fourier transform infrared (FTIR) spectra of BC were obtained on a Perkin Elmer spectrum 100. The powder samples were mixed with KBr of spectroscopic grade and pressed into disks 10 mm in diameter and 1 mm thick. The samples were scanned in the spectral range of 450–4000 cm^{-1}. A scanning electron microscope (SEM, HITACHI S-450 at 10 kV) was employed to examine the surface morphology of the BC before and after adsorption. X-ray diffraction (XRD) patterns were acquired on a Rigaku. D/max-rA (12 kW and Cu K_α radiation).

2.1.2. Adsorbate

The TNT red water provided by the Number 525 ammunition plant (Hubei Province, China) was reddish brown with high COD. The physical and chemical properties of TNT red water diluted 100 times are given in Table 2. The FTIR spectra of TNT red water were measured to study the functional groups.

Different concentrations of solutions were prepared for further dilution and all reagents were of analytical grade.

2.2. Batch treatment of TNT red water

Batch adsorption experiments were conducted using 0.5 g of BC as the adsorbent in a 250 mL flask containing 25 mL of TNT red water. The flasks were agitated at 150 rpm in a temperature-controlled shaker (SHA-BA, Jiangsu, China). The effects of pH were studied in the range of 2.0–12.0 at 303 ± 0.2 K. The pH was adjusted using 0.1 mol/L NaOH and 0.1 mol/L HCl solutions. For investigating the effects of the dilution ratios of TNT red water on adsorption, TNT red water was diluted from 1:50 to 1:600. The effects of temperature and on the BC adsorption capacity were studied at 303, 313, 323, 333, 343 and 353 ± 0.2 K for TNT red water diluted 50–600 times. The effects of contact time on the removal degree of COD from 10 min to 360 min for TNT red water diluted 100 times.

The adsorption isotherms were studied using TNT red water diluted 50–600 times at 303, 313, 323, 333, 343 and 353 ± 0.2 K. The thermodynamics and kinetics were studied using TNT red water diluted 100 times at 303, 313, 323, 333, 343 and 353 ± 0.2K. During the experiment, the BC was removed by carefully filtering the supernatant liquids at various time intervals.

2.3. Chemical oxygen demand analysis (COD)

The COD of TNT red water before and after adsorption were determined by a colorimetric method. The HACH test vials containing potassium dichromate oxidant, catalyst, masking reagent and TNT red water were put into digestion unit (DRB 200, HACH, USA) keeping 120 min at 423 K. After cooling and cleaning the vials, the COD of TNT red water was tested by a DR 2800 spectrophotometer (HACH, USA) at a wavelength of 620 nm in the range of 0–1500 mg/L.

The COD adsorption at equilibrium, q_e (mg/g), and COD removal (%) were calculated as follows:

$$q_e = \frac{(c_0 - c_e)V}{W}, \text{and} \quad (1)$$

$$\text{COD Removal}(\%) = \frac{(c_0 - c_e)}{c_0} \times 100, \quad (2)$$

where c_0 (mg/L) is the initial TNT red water COD and c_e is the equilibrium TNT red water COD, V (L) is the volume of TNT red water and W (g) is the absorbent weight. At any time, the amount of COD adsorbed (mg/g) q_t) by the BC can be calculated using a similar relationship with (1) and the notations were accordingly adapted.

3. Results and discussion

3.1. Characterizations of BC

3.1.1. FTIR analysis of BC

Fig. 1 shows the FTIR spectrum of the BC. The peak at 3649 cm^{-1} is assigned to O–H stretching and that at 2968 cm^{-1} corresponds to $-CH_3$ stretching. The peak at 2332 cm^{-1} corresponds to C≡H stretching whereas the peak at 1720 cm^{-1} can be assigned to –C=O stretching from the carboxylic acid group. The peak at 1080 cm^{-1} can be attributed to the axial deformation vibrations of C–O bonds [17].

3.1.2. SEM and XRD analysis of BC

The surface morphology and characteristics are determined by SEM and XRD. The SEM images of BC (Fig. 2) before and after adsorption show that the BC before adsorption has a porous and coarse surface (Fig. 2a). After adsorption, the porous surface decreases and the BC surface becomes rougher because they are covered by organic materials (Fig. 2b). From Fig. 3 shows XRD spectrum of BC, two broad peaks are observed around 20–27° indicating the lower graphitization degree of BC. Therefore, the BC is an amorphous structure and has a little graphite microcrystal involved [18].

Table 2
Properties of TNT red water diluted 100 times.

pH	COD (mg/L)	Total solids (mg/L)	TNT (mg/L)	2,4-DNT-3-SO_3^- (mg/L)(mg/L)	2,4-DNT-5-SO_3^- (mg/L)	Turbidity	Chromaticity
6.38	850 ± 20	1980	50.7	197	310	59.8	Reddish brown, 1×10^3 times

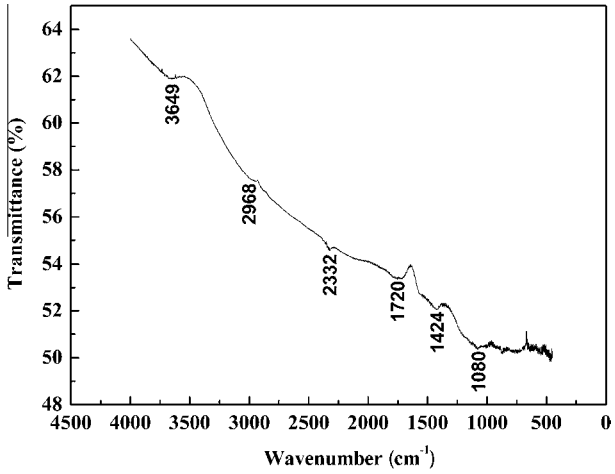

Fig. 1. FTIR spectra for the BC.

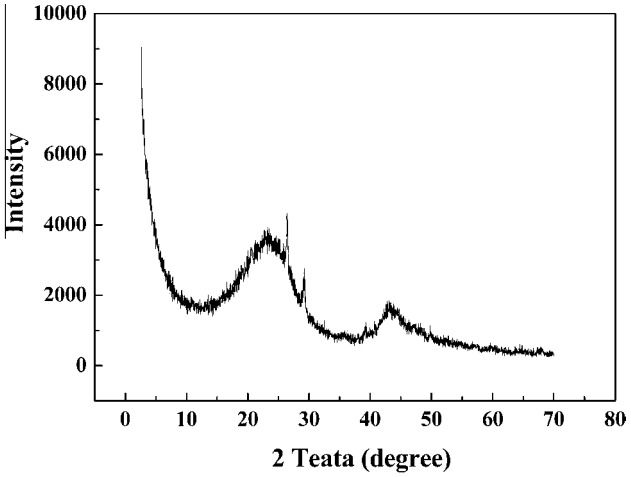

Fig. 3. XRD spectrum of BC.

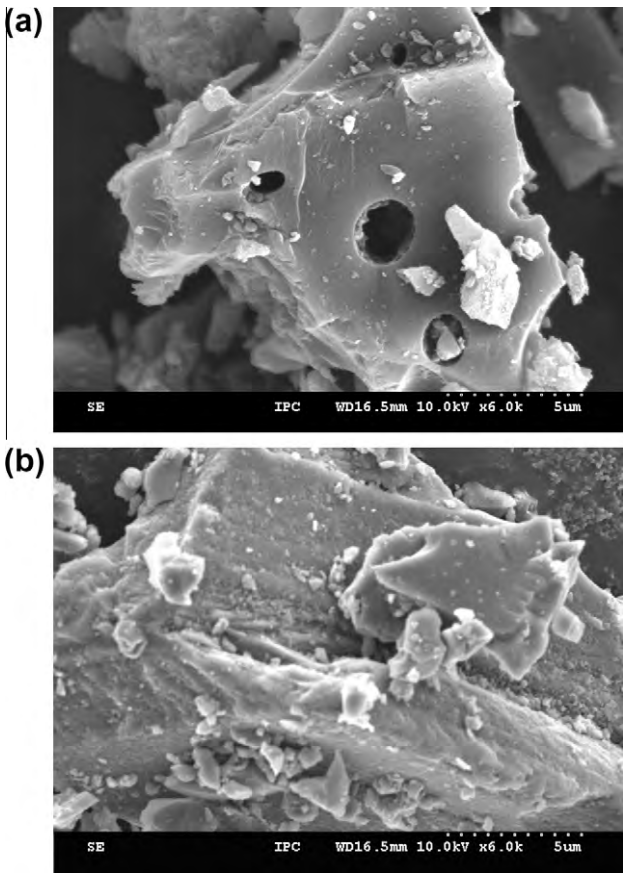

Fig. 2. Scanning electron micrographs of BC at 6000×. (a. before adsorption; b. after adsorption).

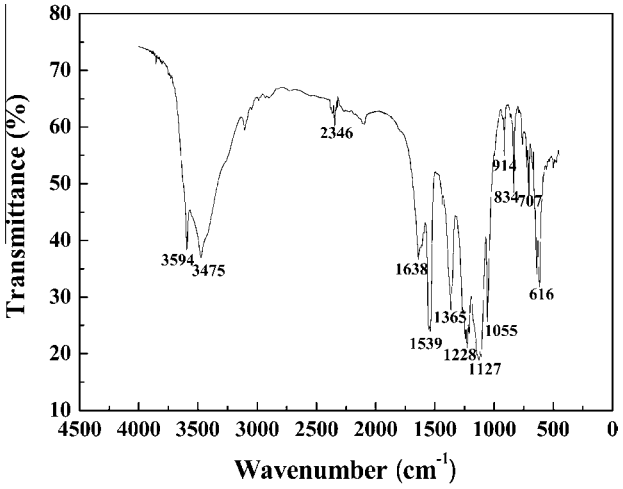

Fig. 4. FTIR spectra for TNT red water.

3.2. FTIR characterizations of TNT red water

Fig. 4 shows the FTIR spectrum of the TNT red water sample after air drying. The adsorption peaks at 3594 and 3475 cm^{-1} are the stretching of the O–H bond of free phenols or those that do not participate in hydrogen bonds, phenols with intermolecular hydrogen bonds .The bands at 1539 and 1365 cm^{-1} can be assigned to $-NO_2$ asymmetric stretching and symmetric stretching and the =C–H plane bending vibration adsorption band at 834 cm^{-1} corresponds to the 2,4,6 substitution of the benzene ring. The =C–H non-plane angle-vibration peak at 707 cm^{-1} is due to1,3 substitution of the benzene ring. The characteristic adsorption peak at 616 cm^{-1} reflects *N*-heterocyclic compounds indicating that nitrogen-containing organic compounds are present in the TNT red water [17].

3.3. Effects of pH on adsorption of organic materials from TNT red water

The pH value is one of the most important physical operational parameter influencing not only solute dissociation from TNT red water, but also the solution chemistry of the organic materials: hydrolysis, complexation by organic, redox reactions, and precipitation are strongly influenced by pH and, on the other side, strongly influence the speciation and the adsorption availability of organic materials [19].

Fig. 5 shows the effects of pH value on the adsorption of organic materials from the TNT red water by the BC. The optimum pH value for organic materials from the TNT red water was determined to be 2.0. The removal degree of COD at the optimum initial pH value was obtained as 82.8%. The main reason is the electrostatic interactions between adsorbent and adsorbate. This is a consequence of the

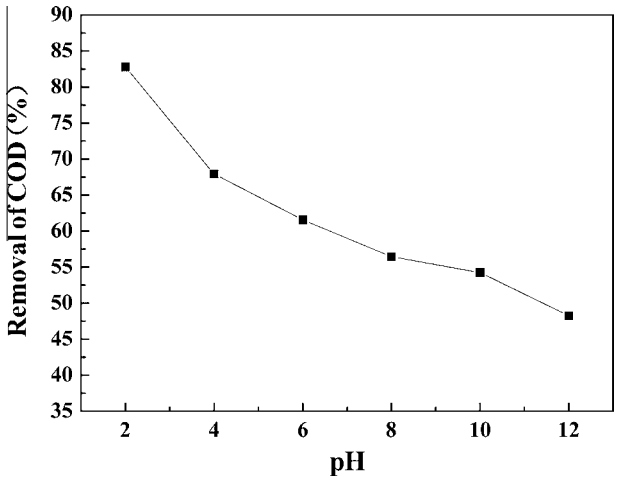

Fig. 5. Effects of pH on adsorption of organic materials from TNT red water (temperature = 303 ± 0.2 K, adsorbent dose = 0.5 g/25 mL, dilution ratio = 1:100 and contact time = 360 min).

complex composition of the TNT red water and the pH_{PZC} of the BC at different pH values. The main components of TNT red water are dinitrotoluene-sulfonate (Ph-SO_3M) and α-TNT. Some α-nitrophenols (NBCs-OH), α-nitrobenzoic acid (NBCs-COOH) and other nitrobenzene compounds (NBCs) are also presented in TNT red water [20]. In the aqueous solution, the dinitrotoluene-sulfonates are dissociated and converted to anionic forms [19]:

$$Ph - SO_3M \overset{H_2O}{\rightarrow} Ph - SO_3^- + M^+ \quad (3)$$

And in an acid medium, most of the organic materials of TNT red water exist in the molecular form because they are difficult to ionize. In a basic medium, α-TNT forms the Janovsky complexes [21] (Scheme 1). And the solubility of α-TNT is low [22]. In addition, the α-nitrophenols and α-nitrobenzoic acid in TNT red water easily ionize to various anionic forms [23], as shown in Eqs. (4) and (5).

$$NBCs - OH \overset{OH^-}{\rightarrow} NCBs - O^- + H_2O \text{ and} \quad (4)$$

$$NBCs - COOH \overset{OH^-}{\rightarrow} NCBs - COO^- + H_2O, \quad (5)$$

Therefore, at pH < pH_{PZC} of BC (pH_{PZC} = 8.21 for BC), the total surface charge of BC is positive leading to the increased removal degree of COD due to the electrostatic force of attraction. Furthermore, the non-polar adsorbent BC tends to adsorb organic materials of molecular form. The lower the pH of the solution is, the more the organic molecules adsorbed. Thence, the removal degree of COD reaches maximum at pH = 2. However, at pH > pH_{PZC}, the BC surface has negative charge and lots of anions involved in TNT red water. Thus the removal degree of COD is smaller because of electrostatic repulsion. And the Janovsky of complexes and the low solubility of α-TNT may bring negative effects on the adsorption.

3.4. Effects of dilution ratios on adsorption of organic materials from TNT red water

Fig. 6 shows that the removal of COD (%) increases from 34.98% to 90.0% as the dilution ratios of TNT red water increases from 1:50 to 1:600. The results can be explained that the organic materials per unit volume of TNT red water decrease with the increasing of dilution ratios. Then the organic materials can adsorb easily on BC resulting in a higher removal of COD. However, an increase of the dilution ratios of TNT red water reduces the diffusion of organic molecules from solution to the adsorbent surface due to the decrease in driving force of the concentration gradient. Hence, the amount of adsorbed COD at equilibrium decreased from 28.66 to 11.52 mg/L as the dilution ratios increased from 1:50 to 1:600.

3.5. Effects of temperature on adsorption of organic materials from TNT red water

The effects of temperature on the adsorption capacity of BC for organic materials are studied at different temperatures (303, 313, 323, 333, 343 and 353 ± 0.2 K) using TNT red water diluted 50–600 times and the results are shown in Fig. 7. The adsorption capacity increases as the temperature increased from 303 to 353 K for all dilution ratios. This suggests that the adsorption process can be controlled by diffusion (intraparticle transport-pore diffusion) and the adsorption process is endothermic [24]. The results can be explained by the increase of mobility in the TNT red water and the decrease of resistance on the diffusing particles at a higher temperature consequently boosting the adsorption capacity. In addition, the higher mobility of molecules facilitates the formation of a surface monolayer at higher temperature [25].

3.6. Effects of contact time on adsorption of organic materials from TNT red water

Fig. 8 shows the effect of the contact time on adsorption of organic materials from TNT red water diluted 100 times at 303, 313, 323, 333, 343 and 353 ± 0.2 K. The adsorption capacity increases quickly during the initial 30 min and then does not change obviously. The adsorption reaches equilibrium at 180 min for all temperatures. It is obvious that a large number of vacant sites on the surface of BC are available during the initial stage of adsorption, and afterward, it is different to occupy the remaining vacant sites due to the repulsive force between the adsorbed molecules on the solid and bulk phases. The similar contact time was reported on adsorption of organic materials from TNT red water using active coke [26]. However, the experimental data were measured at 360 min in order that full equilibrium was reached.

3.7. Adsorption isotherms

The isotherm data obtained at 303, 313, 323, 333, 343 and 353 ± 0.2 K are processed according to the well-known Langmuir, Freundlich, Temkin and Dubinin–Radushkevich isotherm models

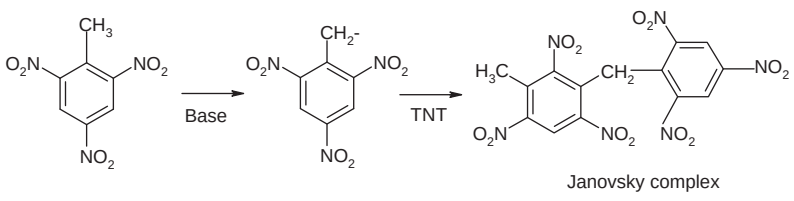

Scheme 1. Formation of Janovsky complexes.

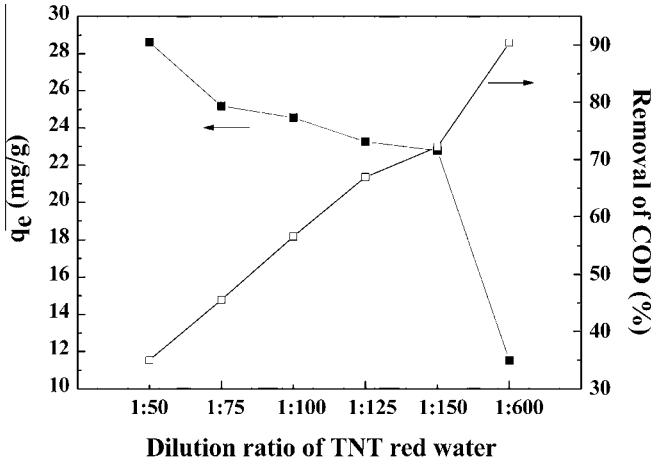

Fig. 6. Effects of dilution ratios of TNT red water on adsorption of organic materials from TNT red water (adsorbent dose = 0.5 g/25mL, temperature = 303 ± 0.2 K and contact time = 360 min).

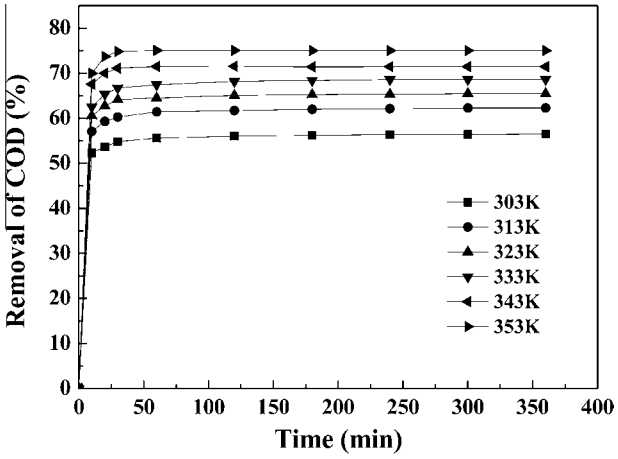

Fig. 8. Effects of contact time on adsorption of organic materials from TNT red water (adsorbent dose = 0.5 g/25 mL, dilution ratio = 1:100 and temperature = 303–353 ± 0.2K).

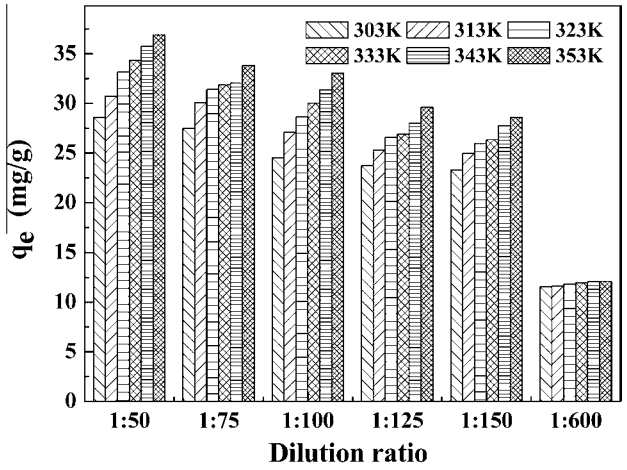

Fig. 7. Effects of temperature on adsorption of organic materials from TNT red water (adsorbent dose = 0.5 g/25 mL, dilution ratio = 1:50–1:600, temperature = 303–353 ± 0.2K and contact time = 360 min).

and the results are presented in Table 3. The Langmuir [27] isotherm equation can be written as follows:

$$q_e = \frac{q_m b c_e}{1 + b c_e} \tag{6}$$

The linear form of Langmuir model is expressed as the following equation:

$$\frac{c_e}{q_e} = \frac{1}{b q_m} + \frac{c_e}{q_m}, \tag{7}$$

where q_e (mg/g) is the amount of COD adsorbed per unit mass by the BC at equilibrium, c_e (mg/L) is the equilibrium TNT red water COD, q_m (mg/g) is the amount of maximum COD adsorbed per unit mass by the BC, and b (L/mg) is the Langmuir adsorption constant. The specific isotherm parameters: q_m and b, are calculated from the slope and intercept of the plots c_e/q_e versus c_e (Fig. 9a), and are listed in Table 3. To determine whether an adsorption system is favorable or unfavorable, R_L, the separation factor, is defined based on the following equation [28]:

$$R_L = \frac{1}{1 + b c_0}, \tag{8}$$

where b (L/mg) is the Langmuir constant and c_0 (mg/L) is the initial TNT red water COD. There are four possible R_L values: $0 < R_L < 1$ characterized a favorable adsorption, $R_L > 1$ characterized an unfavorable adsorption, $R_L = 1$ characterized a linear adsorption, and $R_L = 0$ characterized an irreversible adsorption [29].The R_L values showed in Table 3 indicated a favorable adsorption process for all experimental conditions.

The Freundlich [30] isotherm equation is given as:

$$q_e = K_f c_e^{1/n} \tag{9}$$

The linear form of the Freundlich model is expressed as follows:

$$\log q_e = \log K_f + \frac{1}{n} \log c_e, \tag{10}$$

where q_e is the amount of COD adsorbed per unit mass by the BC at equilibrium (mg/g), c_e (mg/L) is the equilibrium TNT red water COD, and K_f (mg/g (L/mg)$^{1/n}$) and n are Freundlich constant and intensity factors, respectively. The plot of log q_e versus log c_e (Fig. 9b) yields a straight line with a slope of $1/n$.

The Temkin [31] isotherm model is as follows:

$$q_e = \frac{RT}{b} \ln(K_T - c_e) \tag{11}$$

Eq. (11) can be linearized as:

$$q_e = B \ln K_T + B \ln c_e \tag{12}$$

where $RT/b = B$, b and K_T are constants, K_T is the equilibrium binding constant corresponding to the maximum binding energy, and constant B is related to the heat of adsorption. A plot of q_e versus lnc_e (Fig. 9c) enables the determination of the isotherm constant K_T and B.

The Dubinin–Radushkevich (D–R) isotherm [32] is more general because it does not assume a homogenous surface and may distinguish between physical and chemical adsorption. The D–R equation is given as:

$$q_e = q_m \exp(-B\varepsilon^2) \tag{13}$$

$$\text{With } \varepsilon = RT \ln\left(1 + \frac{1}{c_e}\right) \tag{14}$$

where q_m is the adsorption capacity (mol/g), B is a constant related to the adsorption energy (mol^2/kJ^2), and, ε is the Polanyi potential, R is the gas constant (8.314 J/mol K) and T is the absolute temperature. The constant B gives the free energy E (kJ/mol) of the transfer of 1 mol of solute from infinity to the surface of adsorbent and can be computed using the relationship:

Table 3
Parameters of Langmuir, Freundlich, Temkin and Dubinin–Radushkevich isotherm models for organic materials from TNT red water adsorption on BC (Adsorbent dose = 0.5 g/25 mL; Dilution ratio = 1:50–1:600; Temperature = 303–353 ± 0.2K and Contact time = 360min).

Isotherm	Parameters					
	303 K	313 K	323 K	333 K	343 K	353 K
Langmuir						
q_m(mg/g)	29.78	32.19	34.70	37.02	40.23	43.38
b(L/mg)	0.020	0.021	0.019	0.017	0.019	0.018
R_L(1:50)	0.028	0.028	0.030	0.034	0.031	0.033
R_L(1:75)	0.038	0.038	0.040	0.046	0.041	0.044
R_L(1:100)	0.050	0.049	0.052	0.059	0.053	0.057
R_L(1:125)	0.062	0.061	0.064	0.073	0.066	0.070
R_L(1:150)	0.068	0.063	0.071	0.081	0.072	0.078
R_L(1:600)	0.159	0.157	0.164	0.184	0.164	0.178
R^2	0.9995	0.9996	0.9920	0.9977	0.9986	0.9982
Freundlich						
K_f(mg/g(L/mg)$^{1/n}$)	5.72	5.70	5.79	6.12	6.14	5.91
n	4.03	3.80	3.66	3.68	3.43	3.22
R^2	0.9156	0.9097	0.9159	0.9425	0.9334	0.9446
Temkin						
K_T(L/g)	0.61	0.53	0.52	0.52	0.47	0.35
B	4.66	5.21	5.63	5.84	6.64	7.36
R^2	0.9567	0.9544	0.9637	0.9909	0.9789	0.9810
Dubinin–Radushkevich						
q_m (mg/g)	26.07	27.99	29.54	29.64	32.02	30.93
B (mol^2/kJ^2)	83.61	71.65	53.60	36.48	30.81	28.26
E (KJ/mol)	0.08	0.08	0.10	0.12	0.13	0.13
R^2	0.9495	0.9520	0.9464	0.9042	0.8898	0.8664

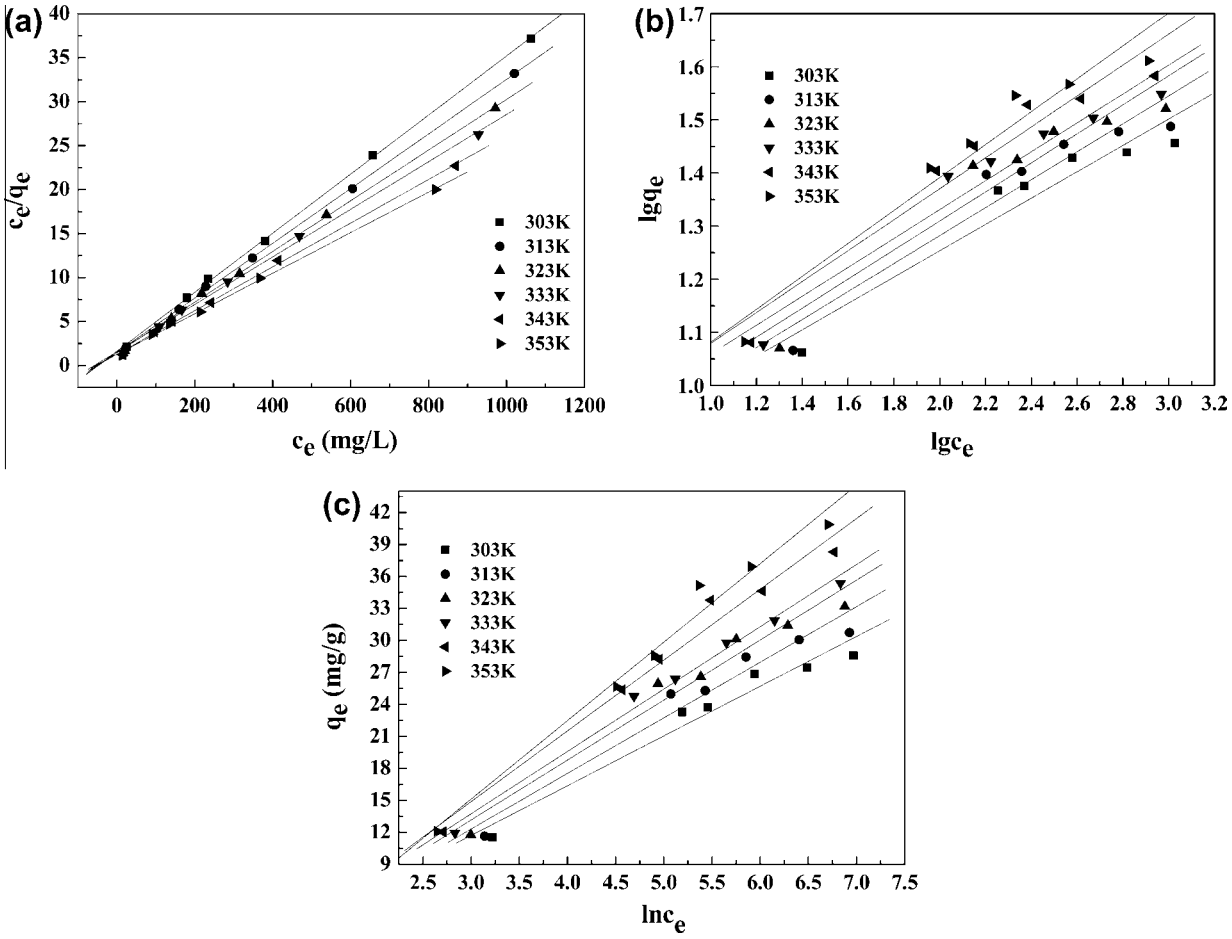

Fig. 9. Adsorption isotherms of organic materials extraction from TNT red water by BC (a) Langmuir adsorption isotherms; (b) Freundlich adsorption isotherms; (c) Temkin adsorption isotherms, adsorbent dose = 0.5 g/25 mL, dilution ratio = 1:50–1:600, temperature = 303–353 ± 0.2 K and contact time = 360 min.

Table 4
Comparison of adsorption capacities of adsorbents and cost analysis toward TNT red water.

Adsorbent	Adsorption capacity (mg COD/g)	Price (CNY/kg)	Adsorption cost (CNY/g COD)	Refs.
Active carbon	10.40	10	0.96	[26]
RS-50B resin	136.00	45	0.33	[26]
Active coke	60.50	0.5	0.0083	[26]
Lignite activated carbon	36.80	4–5	0.11–0.14	[20]
Bamboo charcoal	43.38	1–2	0.023–0.046	Present study

$$E = \frac{1}{\sqrt{-2B}} \tag{15}$$

The D–R equation can be linearized as:

$$\ln q_e = \ln q_m - B\varepsilon^2 \tag{16}$$

A plot of $\ln q_e$ versus ε^2 gave straight lines. The values of q_m (mol/g) and B (mol^2/kJ^2) were obtained from the intercept and slope of the straight line.

The experimental isotherm data are fitted according to the corresponding isotherm equation. Table 3 lists the parameters of the equations and correlation coefficient values. The Langmuir model shows the best fit ($R^2 > 0.99$) compared to the Freundlich and Temkin models under all the experiment conditions. The results may be due to the specific homogeneous nature of the BC surface.

The Temkin isotherm values, B and K_T, (Table 3) indicate that the heat of adsorption of all the molecules in the layer decreases linearly with coverage due to the adsorbent–adsorbate interactions and that adsorption is characterized by a uniform distribution of the binding energies up to the maximum binding energy [33].

The E value from Dubinin–Radushkevich (D–R) isotherm is useful for estimating the type of adsorption and if this value is less than 8 kJ/mol, the adsorption type can be explained by physical adsorption. Otherwise, the adsorption type can be explained by chemical adsorption if this value of E exceeds 8 kJ/ mol [34]. The E values (Table 3) suggest that the adsorption process arises after a physical adsorption mechanism.

Comparative data on the adsorption capacity of BC and the cost analysis with other adsorbents on treat TNT red water reported in the literature are shown in Table 4. These results indicate that BC is comparatively efficient and cheap for the removal of organic materials from TNT red water.

3.8. Adsorption thermodynamics

The adsorption amounts of COD at equilibrium at 3303, 313, 323, 333, 343 and 353 ± 0.2 K are used to calculate the thermodynamics parameters including changes in the free energy (ΔG), enthalpy (ΔH), and entropy (ΔS) according to the following equations [35–37]:

$$K_c = \frac{c_0 - c_e}{c_e} \times \frac{\rho V}{m} = \frac{q_e \rho}{c_e} \tag{17}$$

$$\Delta G = -\mathrm{RT}\ln K_c, \tag{18}$$

$$\ln K_c = \frac{\Delta S}{R} - \frac{\Delta H}{\mathrm{RT}} \tag{19}$$

where K_c is the distribution coefficient, ρ = 1g/L is the density of the solution mixture, c_e is the equilibrium TNT red water COD(mg/L), q_e is the COD amount of adsorption at equilibrium(mg/g), c_{se} is the equilibrium COD in solution (mg/L), T is the solution temperature (K), and R is the gas constant and is equal to 8.314 J/mol K. ΔH and ΔS are calculated from the slope and intercept of the linear plot of $1/T$ versus $\ln K_c$ (figure not shown here). The values of K_c, ΔG, ΔH and ΔS are summarized in Table 5. The changes in the free energy

Table 5
Thermodynamic parameters for adsorption organic materials from TNT red water on BC (Adsorbent dose = 0.5 g/25 mL; Dilution ratio = 1:100; Temperature = 303–353 ± 0.2 K and Contact time = 360 min).

Temperature (K)	K_C	ΔG (KJ/mol)	ΔH (KJ/mol)	ΔS (J/mol K)
303	70.66	−10.73	15.46	85.98
313	81.75	−11.46		
323	96.02	−12.26		
333	104.90	−12.88		
343	147.63	−14.23		
353	164.25	−14.97		

ΔG (negative values of −10.73, −11.46, −12.26, −12.88, −14.23, −14.97 kJ/mol) under the experimental conditions indicate that adsorption of organic materials from the TNT red water is spontaneous. The positive values of ΔH indicate that the adsorption of organic materials on the BC is an endothermic process. In addition, the value of ΔH (15.46 kJ/mol) is between 2 and 40 kJ/mol indicating the physical adsorption characteristics [38]. The entropy change ΔS is positive indicating that the randomness increases during adsorption [39].

3.9. Adsorption kinetics

Lagergren's pseudo-first-order and pseudo-second-order are used to evaluate the kinetics of the adsorption process. The pseudo-first-order kinetic model of Lagergren is [40]:

$$\log(q_e - q_t) = \log(q_e) - k_1 t, \tag{20}$$

where q_e and q_t (mg/g) are the amounts of COD adsorbed (mg/g) at equilibrium and time t (min), respectively and k_1 (1/min) is the rate constant for pseudo-first-order adsorption. When $\log(q_e - q_t)$ is plotted against t k_1 and q_e at different concentrations can be determined from the slope and intercept. The pseudo- second-order equation is expressed as [41]:

$$\frac{t}{q_t} = \frac{1}{k_2 q_e^2} + \frac{1}{q_e} t, \tag{21}$$

where k_2 (g/mg min) is the pseudo second-order constant and q_e and k_2 can be determined experimentally from the slope and intercept of the plot t/q_t versus t.

To compare the validity of each model, a normalized standard deviation Δq (%) is calculated using:

$$\Delta q(\%) = 100\sqrt{\frac{\sum |(q_{exp} - q^{cal})/q_{exp}|^2}{N-1}}, \tag{22}$$

where q_{exp} and q_{cal} (mg/g) are the experimental and calculated amounts of adsorbed COD and N is the number of measurements. If the data from a model are similar to the experimental data, the value of Δq (%) will be small, but if they differ, the value of Δq (%) will be large. To confirm if the adsorption system fits a kinetics model, it is necessary to analyze the data using Δq (%) combined with the determined coefficient R^2.

The kinetic parameters are shown in Table 6. When the correlation coefficients and Δq (%) of the two kinetic models are compared,

Table 6
Parameters of kinetic and Intraparticle diffusion models for organic materials from TNT red water adsorption on BC (Adsorbent dose = 0.5 g/25 mL; Dilution ratio = 1:100; Temperature = 303–353 ± 0.2 K and Contact time = 360 min).

kinetic models	Parameters	303 K	313 K	323 K	333 K	343 K	353 K
Pseudo first-order model	q_e (cal) (mg/g)	3.44	5.33	4.98	4.97	6.25	5.23
	k_1(1/min)	0.015	0.008	0.01	0.016	0.017	0.0168
	R^2	0.5766	0.4616	0.4967	0.7073	0.7464	0.7058
	Δq (%)	94.08	89.02	91.43	92.37	90.13	89.96
Pseudo second-order model	q_e (cal) (mg/g)	26.95	28.51	30.19	31.16	34.45	35.3
	k_2(g/mg min)	0.046	0.018	0.024	0.036	0.028	0.036
	R^2	0.9999	0.9998	0.9997	0.9996	0.9999	0.9999
	Δq (%)	0.53	0.23	0.29	2.1	0.45	0.32
Intraparticle diffusion model	K_{ip1}(mg/g min$^{0.5}$)	0.5018	0.6392	0.7144	0.8378	1.0432	1.2144
	R_1^2	0.9992	0.9791	0.9976	0.9875	0.9823	0.967
	C_1	23.31	23.93	25.24	25.58	26.95	29.07
	K_{ip2}(mg/g min$^{0.5}$)	0.0509	0.0599	0.0567	0.0632	0.0653	0.0681
	R_2^2	0.8669	0.8345	0.9276	0.8675	0.8524	0.9293
	C_2	25.94	27.26	28.95	30.33	33.62	34.42
q_e (exp) (mg/g)		26.85	28.45	30.11	31.77	34.23	35.15

the R^2 values for the pseudo-second-order kinetic model are higher and the values of Δq (%) are lower than R^2 and Δq (%) for the pseudo-first-order kinetic model (Table 6). However, the adsorption capacity for the pseudo-second-order kinetic model is much closer to the experimental value, suggesting that organic materials adsorption by BC follows the pseudo-second-order model.

3.10. Mass transfer models

If the movement of adsorbate from the bulk liquid to the liquid film surrounding the adsorbent is ignored, the adsorption process can be divided into three stages: the first stage is diffusion through the solution to the external surface of the adsorbent which is also called film mass transfer or boundary layer diffusion. The second stage is diffusion within the pores or capillaries of the adsorbent internal structure to the adsorption sites [19]. The third stage is the adsorption of the adsorbate on the internal surface of adsorbent. The last step is assumed to be rapid while stage 1 and 2 are the rate determining steps, either singly or in combination.

3.10.1. Frusawa and Smith model

The external mass transfer coefficients for the organic materials adsorption were determined using a diffusion model referred as the F and S (Frusawa and Smith) model [31]:

$$\ln\left(\frac{c_t}{c_0}-\frac{1}{1+mK_L}\right)=\ln\frac{mK_L}{1+mK_L}-\frac{1+mK_L}{mK_L}\beta_L S_s t \quad (23)$$

where c_t is the concentration after time t (mg/L), c_0 is the initial adsorbate concentration (mg/L), m the mass of adsorbent per unit volume of particle free adsorbate solution (g/L), K_L the Langmuir constant (obtained by multiplying q_m and b) (L/mg), β_L the mass transfer coefficient (cm/s) and S_s is the outer surface of adsorbent per unit volume of particle free slurry (1/cm). In general, the value of S_s is difficult to determine. Then, the $\beta_L S_s$ value was used to describe the adsorption process [42,43].

The plot of $\ln(c_t/c_0-(1/1+mK_L))$ versus t for adsorption organic materials at various temperatures is shown in Fig. 10. The value $\beta_L S_s$ was calculated from the slope of the straight line plot in Fig. 9 and was found to be as 2.87×10^{-6}, 1.04×10^{-5}, 9.88×10^{-6}, 7.83×10^{-6},1.61×10^{-5} and 1.22×10^{-5}1/s for organic materials at all temperatures. This value indicates that the velocity of organic materials transport from liquid phase to the surface of BC is rapid enough to remove organic materials from TNT red water by BC. The same conclusion was obtained by Özer et al. and Panday et al. [19,42].

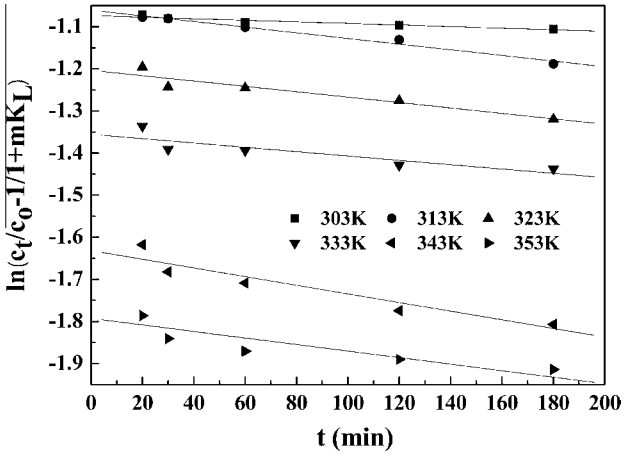

Fig. 10. Mass transfer plot for the adsorption of organic materials on BC.

3.10.2. Intraparticle diffusion model (Weber-Morris model)

In order to investigate the mechanism of organic materials adsorption from TNT red water and potential rate-controlling steps such as external mass transfer, intraparticle diffusion and adsorption processes, Weber–Morris model is used to test the experimental data.

The intraparticle diffusion equation can be presented as follows [44]:

$$q_t = k_{pi}t^{1/2} + c_i, \quad (24)$$

where k_{pi} (mg/g min$^{1/2}$) is the intraparticle diffusion rate constant at stage i, and c_i is the intercept at stage i.

Fig. 11 shows the pore diffusion plot of organic materials adsorption by the BC at 303, 313, 323, 333, 343 and 353 ± 0.2 K. The corresponding model parameters are listed in Table 6. If the plot passes through the origin, the plot of q_t versus $t^{1/2}$ will be linear and then the rate controlling step is only intraparticle diffusion, otherwise, another mechanism together with intraparticle diffusion is involved. As shown in Fig. 11, the linear portions of the curves do not pass through the origin indicating that the intraparticle diffusion was not the only rate-limiting step. The mechanism of organic materials from TNT red water on BC is complex and both the surface adsorption as well as intraparticle diffusion contributes to the actual adsorption process. The first sharper portion in Fig. 11 is assigned to the external surface adsorption or instantaneous adsorption and the second portion shows gradual adsorption

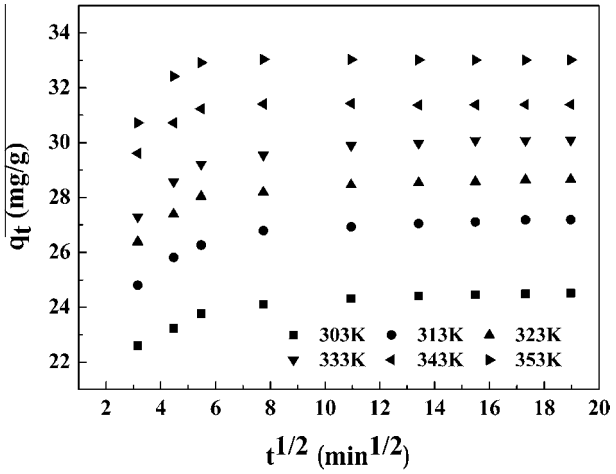

Fig. 11. Intraparticle diffusion kinetics for organic materials adsorption from TNT red water by BC (absorbent dosage = 0.5 g/25 mL, ratio of dilution = 1:100, temperature = 303–353 ± 0.2K and contact time = 360 min).

where intraparticle diffusion is rate-limiting [45]. At all the temperatures, k_{p1} is larger than k_{p2}, indicating that the adsorption efficiency is higher in the beginning due to the large number of vacant sites on the BC surface. After the adsorbed materials form a thick layer, the capacity is exhausted and the adsorption efficiency is controlled by the rate at which the adsorbent is transported from the exterior to the interior sites of the adsorbent. The intercept c_i gives an idea about the thickness of the boundary layer, and the larger the intercept the greater is the boundary layer effect. The c_i values listed in Table 6 indicate that the adsorption process is affected by the boundary layer .That is, the effect of the external mass transfer resistance on the process of diffusion cannot be neglected [19].

3.11. Mechanisms of adsorption

The mechanisms of adsorption process are also related to the electrostatic interactions, hydrogen bonding formation, electron donor–acceptor interaction, and π–π dispersion interaction [17]. In our previous analyses, electrostatic interactions have become the major factor by discussing on the effect of pH on the adsorption. The physical forces such as hydrogen bonding interaction between organic materials and BC act as the dominant role in the adsorption process because the value of ΔH is 15.46 kJ/mol from the thermodynamic analyses [38]. The results can be explained by the functional groups present on the surface of BC and in the TNT red water. As demonstrated by the results of Boehm's titration (Table 1) and FT-IR analysis, the main adsorption groups of the BC are carboxylic, phenolic groups, and lactonic groups. The hydrogen atoms of these groups in BC can form hydrogen bonding with nitrogen and oxygen atoms from the NBCs of TNT red water (Scheme 2a). On the other hand, the oxygen of the groups in the BC can also act by hydrogen bonding with hydrogen atoms of −COOH, −OH, HSO_3^- and $-NH_2$ from the NBCs of TNT red water (Scheme 2.b). The *n*–π donor acceptor interaction [46] can be concluded between the electron pair of carbonyl O acting as the donor and the π-acceptor of aromatic compounds (α-TNT, α-itrophenols, α-nitrobenzoic acid and other nitrobenzene compounds). π–π dispersion interaction can present between the aromatic ring of organic compounds and the structure of graphite layer with enclosed π electron or the adsorbent with aromatic structure [47,48]. The facts have been concluded that most of the organic materials in the TNT red water have aromatic rings structures [20], but the XRD showed that BC is an amorphous structure. Therefore, the mechanism of π–π dispersion interaction should be ignored in the study of adsorption processes.

Based on the previous analysis, the mechanisms of adsorption are also related with the carboxylic, phenolic and lactonic functional groups on the surface of BC (Table 1). The influence of the structure of BC is ruled out.

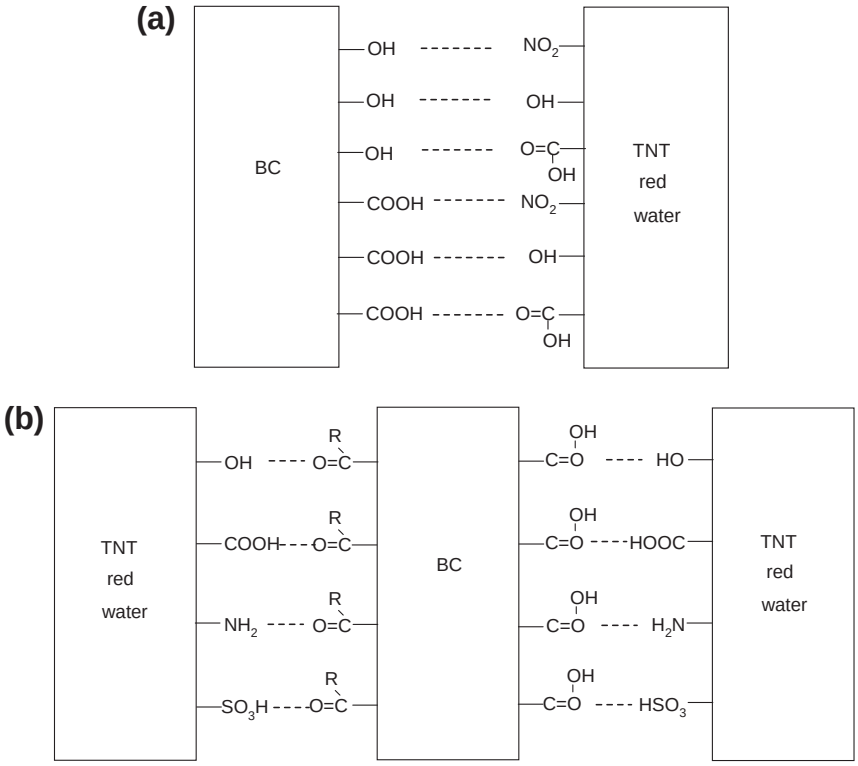

Scheme 2. The models of hydrogen bonding between Bamboo Charcoal and organic materials of TNT red water.

4. Conclusion

BC is an effective adsorbent for the removal of organic materials from TNT red water. The pH value and the dilution ratios of TNT red water obviously influenced the adsorption process. The equilibrium adsorption data are best fitted by Langmuir isotherm. The D–R isotherms further suggest the physical adsorption mechanism of adsorption organic materials from TNT red water. The adsorption kinetics is found to follow a pseudo-second-order model. Thermodynamic analyses indicate that adsorption of organic materials from TNT red water by BC is an endothermic, spontaneous process and the randomness at the solid/solution interface increases at all the temperatures tested. The results of Frusawa and Smith diffusion models indicate that the velocity of organic materials transport from the liquid phase to the surface of BC is rapid. The Weber–Morris model shows that the intraparticle diffusion was not the only rate-limiting step. The mechanism of organic materials from TNT red water on BC is complex and both the surface adsorption as well as intraparticle diffusion contributes to the actual adsorption process. The adsorption mechanisms are also related with electrostatic interaction, hydrogen bonding formation, and electron donor–acceptor interaction. BC shows excellent adsorption characteristics and can be used in the removal of organic materials from TNT red water.

Acknowledgements

This research was jointly supported by National High Technology Research and Development Program (863 Program 2012AA06A109) of China, the Fundamental Research Funds for the Central Universities (2010ZD08), the special co-construction project of Beijing city education committee, Doctoral Program Foundation of Institution of higher education of China(2-2-08-07), and City University of Hong Kong Strategic Research Grant (SRG) No. 7008009.

References

[1] A. Kaidar, D.H. Eric, C. Michel, B. Alain, Application of advanced oxidation processes for TNT removal: a review, J. Hazard. Mater. 178 (2010) 10–28.
[2] Q.L. Zhao, Z.F. Ye, M.H. Zhang, Treatment of 2,4,6-trinitrotoluene (TNT) TNT red water by vacuum distillation, Chemosphere 80 (2010) 947–950.
[3] E.K. Nefso, S.E. Burns, C.J. McGrath, Degradation kinetics of TNT in the presence of six mineral surfaces and ferrous iron, J. Hazard. Mater B. 123 (2005) 79–88.
[4] G. Adamia, M. Ghoghoberidze, D. Graves, G. Khatisashvili, G. Kvesitadze, E. Lomidze, D. Ugrekhelidze, G. Zaalishvili, Adsorption, distribution, and transformation of TNT in higher plants, Ecotox. Environ. Safe. 64 (2006) 136–145.
[5] F.Q. An, B.J. Gao, X.Q. Feng, Adsorption performance and mechanism of 2,4,6-trinitrotoluene on a novel adsorption material polyvinylbenzyl acid/SiO_2, Appl. Surf. Sci. 255 (2009) 5031–5035.
[6] W.S. Chen, W.C. Chiang, K.M. Wei, Recovery of nitrotoluenes from wastewater by solvent extraction enhanced with salting-out effect, J. Hazard. Mater. 147 (2007) 197–204.
[7] S. Hwang, E.J. Bouwer, S.L. Larson, J.L. Davis, Decolorization of alkaline TNT hydrolysis effluents using UV/H_2O_2, J. Hazard. Mater. 108 (2004) 61–67.
[8] S.V. Muhammad, T. Keiichi, Photocatalytic degradation of nitrotoluene in aqueous TiO_2 suspension, Water Res. 36 (2002) 59–64.
[9] R. Matta, K. Hanna, T. Kone, Oxidation of 2,4,6-trinitrotoluene in the presence of different iron-bearing minerals at neutral pH, Chem. Eng. J. 144 (2008) 453–458.
[10] S.W. Maloney, N.R. Adrian, R.F. Hickey, Anaerobic treatment of pink water in a fluidized bed reactor containing GAC, J. Hazard Mater. 92 (2002) 77–88.
[11] I. Abe, T.O. Fukuhara, J. Maruyama, H. Tatsumoto, S. Iwasaki, Preparation of carbonaceous adsorbents for removal of chloroform from drinking water, Carbon 39 (2001) 1069–1073.
[12] S.Y. Wang, M.H. Tsai, S.F. Lo, M.J. Tsai, Effects of manufacturing conditions on the adsorption capacity of heavy metal ions by Makino bamboo charcoal, Bioresource Technol. 99 (2008) 7027–7033.
[13] K. Mizuta, T. Matsumoto, Y. Hatate, K. Nishihara, T. Nakanish, Removal of nitrate-nitrogen from drinking water using bamboo powder charcoal, Bioresource Technol. 95 (2004) 255–257.
[14] M. Wang, Z.H. Huang, G.J. Liu, F.Y. Kang, Adsorption of dimethyl sulfide from aqueous solution by a cost-effective bamboo charcoal, J. Hazard. Mater. 190 (2011) 1009–1015.
[15] C. Namasivayam, D. Sangeetha, Removal and recovery of vanadium (V) by adsorption onto $ZnCl_2$ activated carbon: kinetics and isotherms, Adsorption 12 (2006) 103–117.
[16] J.S. Noh, J.A. Schwarz, Estimation of the point of zero charge of simple oxides by mass titration, J. Colloid Interf. Sci. (1990) 130–157.
[17] Alexandro M.M. Vargas, André L. Cazetta, Marcos H. Kunita, Taís L. Silva, Vitor C. Almeida, Adsorption of methylene blue on activated carbon produced from flamboyant pods (Delonix regia): study of adsorption isotherms and kinetic models, Chem. Eng. J. 168 (2011) 722–730.
[18] Y.C. Changa, H.J. Sohna, Y.Z. Koraib, I. Mochida, Anodic performances of coke from coals, Carbon 36 (1998) 1653–1662.
[19] A. Özer, G. Akkaya, M. Turabik, Biosorption of Acid Blue 290 (AB 290) and Acid Blue 324. (AB 324) dyes on Spirogyra rhizopus, J. Hazard. Mater B. 135 (2006) 355–364.
[20] F.F. Wei, Y.H. Zhang, F.Z. Lv, P.K. Chu, Z.F. Ye, Extraction of organic materials from red water by metal-impregnated lignite activated carbon, J. Hazard. Mater.197 (2011) 352-360.
[21] J.P. Zhang, X.Y. Lin, X.G. Luo, C. Zhang, H. Zhu, A modified lignin adsorbent for the removal of 2,4,6-trinitrotoluene, Chem. Eng. J. 168 (2011) 1055–1063.
[22] S. Ro Kyoung, Asha Venugopal, D. Dean Adrian, David Constant, Kamel Qaisi, Kalliat T. Valsaraj, Louis J. Thibodeaux, Dipak Roy, Solubility of 2,4,6-Trinitrotoluene (TNT) in Water, J. Chem. Eng. Data. 41 (1996) 758–761.
[23] F.Y. Wang, H. Wang, J.W. Ma, Adsorption of cadmium (II) ions from aqueous solution by a new low-cost adsorbent—Bamboo charcoal, J. Hazard. Mater. 177 (2010) 300–306.
[24] C.V. Srivastava, M.M. Swamy1, D.I. Mall, P. Basheswar, M.I. Mishra, Adsorptive removal of phenol by bagasse fly ash and activated carbon: equilibrium, kinetics and thermodynamics, Colloids Surf. A: Physicochem. Eng. Aspects 272 (2006) 89–104.
[25] N. Nasuha, B.H. Hameed, T. Azam, M. Din, Rejected tea as a potential low-cost adsorbent for the removal of methylene blue, J. Hazard. Mater. 175 (2010) 126–132.
[26] M.H. Zhang, Q.L. Zhao, Z.F. Ye, Organic pollutants removal from 2,4,6-trinitrotoluene (TNT) red water using low cost activated coke, J. Environ. Sci. 23 (2011) 1962–1969.
[27] S. Karagöz, T. Tay, S. Ucar, M. Erdem, Activated carbons from waste biomass by sulfuric acid activation and their use on methylene blue adsorption, Bioresource Technol. 99 (2008) 6214–6222.
[28] Y.J. Yao, F.F. Xu, M. Chen, Z.X. Xu, Z. Zhu, Adsorption behavior of methylene blue on carbon nanotubes, Bioresource Technol. 101 (2010) 3040–3046.
[29] K. Saltalı, A. Sarı, M. Aydın, Removal of ammonium ion from aqueous solution by natural Turkish zeolite for environmental quality, J. Hazard. Mater. 141 (2007) 258–263.
[30] H.M.F. Freundlich, Über die adsorption in lösungen, Zeitschrift fur Physikalische Chemie (Leipzig) 57A (1906) 385–470.
[31] K.K.H. Choy, G. McKay, J.F. Porter, Sorption of acid dyes from effluents using activated carbon, Resour. Conserv. Recy. 27 (1999) 57–71.
[32] K. Saltalı, A. Sarı., M. Aydın, Removal of ammonium ion from aqueous solution by natural Turkish zeolite for environmental quality, J. Hazard. Mater. 141 (2007) 258–263.
[33] D. Harikishore Kumar Reddy, K. Seshaiaha, A.V.R. Reddy, M. Madhava Rao, M.C. Wang, Biosorption of Pb2+ from aqueous solutions by Moringa oleifera bark: Equilibrium and kinetic studies, J. Hazard. Mater. 174 (2010) 831–838.
[34] Z. Aksu, Determination of equilibrium, kinetic and thermodynamic parameters of the batch biosorption of nikel ions onto C vulgaris, Process Biochem. 38 (2002) 89–99.
[35] B. Kannamba, K. Laxma Reddy, D.B.V. AppaRao, Removal of Cu (II) from aqueous solutions using chemically modified chitosan, J. Hazard. Mater. 175 (2010) 939–948.
[36] A. Kumar, B. Prasad, I.M. Mishra, Adsorptive removal of acrylonitrile by commercial grade activated carbon: Kinetics, equilibrium and thermodynamics, J. Hazard. Mater. 152 (2008) 589–600.
[37] H. Zhang, X.J. Yu, L. Chen, J.Q. Geng, Investigation of radionuclide 63 Ni(II) sorption on ZSM-5 zeolite, J. Radioanal. Nucl. Chem. 286 (2010) 249–258.
[38] V.B. Oepen, W.K. Ordel, W. Klein, Sorption of nonpolar and polar compounds to soils: processes, measurement and experience with the applicability of the modified OECD-guideline, Chemosphere 22 (1991) 285–304.
[39] H. Zheng, L.J. Han, H.W. Ma, Y. Zheng, H.M. Zhang, D.H. Liu, S. Liang, Adsorption characteristics of ammonium ion by zeolite 13×, J. Hazard. Mater. 158 (2008) 577–584.
[40] S. Lagergren, About the theory of so-called adsorption of soluble substances, K. Svenska Vetenskapsakad Handl. 24 (1898) 1–39.
[41] Y.S. Ho, G. McKay, Pseudo-second order model for sorption processes, Process Biochem. 34 (5) (1999) 451–465.
[42] K.K. Panday, G. Prasad, V.N. Singh, Use of wollastonite for the treatment of Cu(II) rich effluents, Water Air Soil pollut. 27 (1986) 287–296.
[43] A. Özer, G. Akkaya, M. Turabik, The biosorption of Acid Red 337 and Acid Blue 324 on Enteromorpha prolifera: the application of nonlinear regression analysis to dye biosorption, Chem. Eng. J. 112 (2005) 181–190.
[44] W.J. Weber Jr, J.C. Morris, Kinetics of adsorption on carbon from solution, J. Sanit. Eng. Div. 89 (1963) 31–59.

[45] F.C. Wu, R.L. Tseng, R.S. Juang, Comparisons of porous and adsorption properties of carbons activated by steam and KOH, J. Colloid Interf. Sci. 283 (2005) 49–56.
[46] J.S. Mattson, H.B.J. Mark, M.D. Malbin, W.J. Weber, J.C. Crittenden, Surface chemistry of active carbon: specific adsorption of phenols, J. Colloid Int. Sci. 31 (1969) 116–130.
[47] D.Q. Zhu, Seokjoon Kwon, Joseph J. Pignatello, Adsorption of single-ring organic compounds to wood charcoals prepared under different thermochemical conditions, Environ. Sci. Technol. 39 (2005) 3990–3998.
[48] C. Moreno-Castilla, Adsorption of organic molecules from aqueous solutions on carbon materials, Carbon 42 (2004) 83–94.